

Analytical and higher order finite element hybrid approach for an efficient simulation of ultrasonic guided waves I: 2D-analysis

Juan M. Vivar-Perez^{*1}, Sascha Duczec^{2a} and Ulrich Gabbert^{2b}

¹German Aerospace Center (DLR), Institute of Composite Structures and Adaptive Systems,
Sportallee 54a, 223355 Hamburg, Germany

²Otto-von-Guericke University of Magdeburg, Institute of Mechanics,
Universitätsplatz 2, 39106 Magdeburg, Germany

(Received April 2, 2013, Revised December 11, 2013, Accepted December 12, 2013)

Abstract. In recent years the interest in online monitoring of lightweight structures with ultrasonic guided waves is steadily growing. Especially the aircraft industry is a driving force in the development of structural health monitoring (SHM) systems. In order to optimally design SHM systems powerful and efficient numerical simulation tools to predict the behaviour of ultrasonic elastic waves in thin-walled structures are required. It has been shown that in real industrial applications, such as airplane wings or fuselages, conventional linear and quadratic pure displacement finite elements commonly used to model ultrasonic elastic waves quickly reach their limits. The required mesh density, to obtain good quality solutions, results in enormous computational costs when solving the wave propagation problem in the time domain. To resolve this problem different possibilities are available. Analytical methods and higher order finite element method approaches (HO-FEM), like p-FEM, spectral elements, spectral analysis and isogeometric analysis, are among them. Although analytical approaches offer fast and accurate results, they are limited to rather simple geometries. On the other hand, the application of higher order finite element schemes is a computationally demanding task. The drawbacks of both methods can be circumvented if regions of complex geometry are modelled using a HO-FEM approach while the response of the remaining structure is computed utilizing an analytical approach. The objective of the paper is to present an efficient method to couple different HO-FEM schemes with an analytical description of an undisturbed region. Using this hybrid formulation the numerical effort can be drastically reduced. The functionality of the proposed scheme is demonstrated by studying the propagation of ultrasonic guided waves in plates, excited by a piezoelectric patch actuator. The actuator is modelled utilizing higher order coupled field finite elements, whereas the homogenous, isotropic plate is described analytically. The results of this "semi-analytical" approach highlight the opportunities to reduce the numerical effort if closed-form solutions are partially available.

Keywords: analytical methods; spectral finite elements; higher order finite elements; piezoelectricity; structural health monitoring; Lamb waves

*Corresponding author, Dr.-Ing., E-mail: Juan.VivarPerez@dlr.de

^a Ph. D. Student, E-mail: Sascha.Duczec@ovgu.de

^b Prof. Dr.-Ing., E-mail: Ulrich.Gabbert@ovgu.de

1. Introduction

Guided structural wave inspection methods in thin plate-like structures involve necessarily the use of Lamb waves. These kind of elastic waves have several good properties. According to Raghavan and Cesnik (2007), its amplitude decay ratio is less than that of sonic waves emitted outside the structure and their propagation velocity is higher according to Rose (2002). When excited at high frequencies, they have a very short wave length which makes them very sensitive to small perturbations of the plate-like structure and, at the same time, different modes can be induced. These features allow scanning a bigger area of the structure, to localize relatively small damages, to characterize the localized damages in accordance to its interaction with each mode (Willberg *et al.* 2009a) and to scan not only the surface, but also through the thickness of the structure. These facts are what make Lamb-wave-based structural online monitoring systems very attractive for the SHM research community (Wang *et al.* 2008, Lu *et al.* 2008).

In active SHM systems Lamb waves need to be excited and monitored. A mean to do this is through the use of piezoelectric transducers. Piezoelectric patches are bonded to the structure, allowing the excitation and sensing of Lamb waves through the use of the inverse and direct piezoelectric effect (see Fig. 1). This is one of the most used type of sensors and actuators due to their relatively easy integration in to the structure and their low costs (Wang *et al.* 2008, Lu *et al.* 2008).

In spite of their good capabilities and promising features, the use of Lamb waves for SHM applications has also some difficulties. The use of Lamb waves to detect damages is what is called an inverse problem. In general terms, inverse problems are ill-conditioned and very difficult to solve (Bonnet and Constantinescu 2005, Leonard *et al.* 2002, Chakraborty and Gopalakrishnan 2004). An excitation pulse normally consists of several modes that convert into each other in the presence of structural changes as well as damages and are superposed making the obtained wave signals very complex to analyze (Ahmad 2011). The high propagation velocity implies that reflections from structural boundaries contribute to the received wave signals at the sensors. Thus, information related to structural damages is hard to identify due to the complexity of the signals (Su and Ye 2009).

To overcome these difficulties, a good understanding of the wave propagation through the structure is essential.

An appropriate theoretical reference model is indispensable in order to elucidate the main features that characterize Lamb waves, to apply this knowledge to interpret the sensors signals, to design optimal excitation profiles and to distinguish which kind of excitation is adequate for each application.

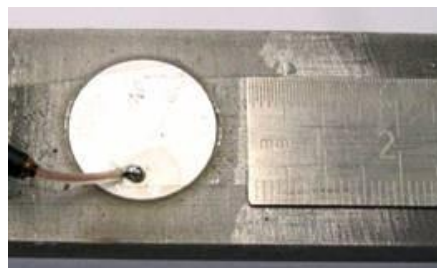


Fig. 1 Piezoelectric patch used as a transducer. Piezoelectric transducers can be used as actuators as well as sensors. They are very popular due to their relatively easy integration and low cost

The beginning of the theoretical studies of Lamb waves can be set in 1889 with Lord Rayleigh, who first modeled the elastic wave propagation along a guided surface of an isotropic homogeneous semi-infinite solid (Rayleigh 1885). These waves are known today as surface or *Rayleigh* waves. Love (1911) added another parallel surface in order to simulate horizontally polarized waves, termed *SH* waves. Based on the work of Lord Rayleigh, Horace Lamb (1917) published his seminal work "On Waves in an Elastic Plate". Lamb studied the propagation of guided waves between two parallel plane surfaces with polarization of displacements parallel and perpendicular to the direction of propagation. After the publication of this work, elastic waves in thin isotropic plates were named after him.

Lamb's problem was again retaken, when Osborne and Hart (1945) studied Lamb waves excited by underwater explosions. At this point, the final solution of the field of displacements demanded to solve the Rayleigh-Lamb dispersion equation. Upper and lower bounds together with asymptotic methods were used by Holden (1951) and Mindlin (1951), and later extended by Onoe (1955) to describe a qualitative behavior of the real branches of the Lamb wave dispersion curves corresponding to propagating Lamb modes. The computation of bounds and the qualitative behavior of imaginary branches corresponding to evanescent Lamb modes were first performed by Lyon (1955). The existence of complex branches and their corresponding phase velocities for real frequencies were established by Mindlin and Medick (1959). Later a comprehensive solution of the dispersion equation for each Lamb wave mode was given by Mindlin (1960). Gazis (1958) using a digital computer gave approximated solutions to the dispersion equation corresponding to propagating modes, which were computed more accurately with more computation power by Viktorov (1967). Viktorov also analyzed the problem of forced motion in the two-dimensional case. In all these previous studies, the plain strain condition was always assumed, leading to a two-dimensional formulation of the problem.

Achenbach (1973) also presented a study on the forced motion and the response of a plate under vertical point forces applied on the surface. Graff (1975) extended the aforementioned work to the three dimensional case by studying circular crested waves.

In the last decades Lamb waves have found an application in non-destructive testing. Consequently, the effort to model elastic waves in plates has been multiplied. We can refer to the publications of Achenbach (1998, 1999, 2000, 2003) and Achenbach and Xu (1999), where the concept of the membrane carrier wave together with mechanical reciprocity is used to describe the field of displacements in isotropic plates. Some work has also been done using the Fourier transform and the Cauchy's theorem of residues in the works of Gomitko *et al.* (1991), Raghavan and Cesnik (2004), Giurgiutiu (2005), von Ende *et al.* (2007) and von Ende and Lammering (2007, 2009). In the work of Wilcox (2004), the excitation matrices are defined to model Lamb wave fields excited by line and point distribution of forces. The modal analysis has also been considered in order to obtain analytical solutions, as in the work of Jin *et al.* (2003). Another analytical approach is the use of the Green's tensor for point forces in the surface of the three-dimensional model of the plate. This can be seen in the works of Karmazin *et al.* (2010, 2011) and Glushkov *et al.* (2006, 2010). Some hybrid approaches have also been formulated as in the work of Velichko and Wilcox (2007) where the Green's function for a laminated plate is obtained using modal analysis.

Parallel to the analytical approaches mentioned above, other numerical and semi-analytical approaches have been used to model Lamb waves such as the Finite Difference Method as in the work from Sun and Wu (2009), the Local Interaction Simulation Approach as in the works from Delsanto *et al.* (1992, 1994, 1997) and Lee and Staszewski (2003a, b) the Finite Element Method

(Willberg *et al.* 2009a, b, Xu *et al.* 2004), the Spectral Analysis (Vivar-Perez *et al.* 2009a, b), the Spectral Element Method in the time domain (Ostachowicz *et al.* 2012, Peng *et al.* 2009, Kudela and Ostachowicz 2008, 2009), the Spectral Element Method in the frequency domain with the use of the Fast Fourier or the Wavelet Transform (Doyle 1997, Gopalakrishnan *et al.* 2008, Gopalakrishnan and Mitra 2012) as well as the Semi-Analytic Finite Element Method (Ahmad 2011, Ahmad *et al.* 2009, Bartoli *et al.* 2006, Galán and Abascal 2002). A nice comparison and overview of different higher order finite element formulations applied to the modeling of Lamb wave propagation can be found in Duczek *et al.* (2012) and Willberg *et al.* (2012). Some mixed formulations have been applied as well in order to keep advantages and decrease disadvantages of different methods such as by a combination of semi-analytic finite elements and standard finite elements as in Ahmad (2011) and Liu (2002), and also by a combination of some analytical methods with finite element solutions as in Tian *et al.* (2004) and Vivar-Perez (2012), to mention just a few.

The application of analytical methods is very convenient in the simulation of Lamb waves since their evaluation is relatively inexpensive from a numerical point of view. Furthermore, the qualitative behavior of Lamb wave propagation can be derived by analytical expressions. They have the disadvantage of being only developed for specific geometries, and mostly they are only given in the frequency domain. The direct application of purely numerical methods such as the Finite Element Method is the most commonly used approach due to their flexibility to model arbitrary geometries. However, it is the most expensive method in terms of computational effort, since the number of elements and degrees of freedoms in the model increase in regions of abrupt changes in material properties or in cases of rapid variation of the solution in very small subdomains of the integration domain, as in the case of modeling ultrasonic Lamb waves.

Our approach to model Lamb-wave-based SHM systems is a hybrid formulation that deploys an analytical solution in regular regions of the structure and applies discrete approximation models in regions where the plate-like structure is perturbed. Hence, this paper constitutes a contribution to the mathematical description and numerical modeling of elastic waves in thin plates.

To reach our goal we used a procedure already exploited in the published works by Karmazin *et al.* (2010, 2011) and Gluskov *et al.* (2006, 2010). In these works, the problem of the wave propagation in a plate is analyzed in the frequency domain. For the system of partial differential equations in frequency domain the fundamental solution or Green's tensor is found with the help of Cauchy's residues theorem. We derive integral expressions which can be used to find the response of the plate under an arbitrary distribution of loads in a localized region of the surface of the plate. Although it is not presented here, the obtained formulas can be used in the same way as Ahmad (2011) and Morvan *et al.* (2003) to describe the reflected waves originated from boundaries and defects of the plate.

We are mainly interested in the excitation and reception of waves by piezoelectric actuators and sensors, respectively (Sirohi and Chopra 2000). For that reason, it is of great significance to provide mathematical tools that consider the electro-mechanical coupling effect of actuators and sensors bonded to the plate and their influence to the structure (Huand and Derriso 2008). These tools should be able to model the wave reflections caused by defects or perturbations from the geometry of the plate-like structure as well (Ahmad 2011, Ahmad *et al.* 2009).

The novel contribution is that this aim was reached using Chebyshev spectral analysis in the frequency domain to model any perturbation of the plate geometry instead of the classical Finite Element Method used by Chang and Mal (1999) and Hayashi and Kawashima (2002). Spectral analysis has a higher order of accuracy than standard finite elements as it has been shown in the

works of Boyd (2000), Fornberg (1998) and Trefethen among others. Also as a novelty, the bonding condition between the piezoelectric patch and the plate in the frequency domain is given in an analytical way, and finally, with the help of quadrature formulas and spectral analysis, the set of coupling equations were discretized and semi-analytical expressions for the propagation of Lamb waves were obtained using the concept of the dynamic reaction or response matrix of the plate with exact wavenumbers. The implied advantage of using exact wavenumbers instead of approximated ones is that it increases the level of accuracy of the final results and no discretization through the thickness of the plate has to be used as in the works presented by Loveday (2007), Ahmad (2011) or Morvan *et al.* (2003).

2. Statement of the problem

The main purpose of this work is to model ultrasonic elastic waves induced and received by piezoelectric patches bonded to an isotropic plate. It is considered that a piezoelectric patch occupies a domain Ω and is bonded to an infinite isotropic plate. The piezoelectric transducer and the plate share the common surface Γ . A schematic representation of the problem under consideration is displayed in Fig. 2.

We analyze the governing equations of the piezoelectric patch and of the plate separately. The bonding conditions on the interface Γ will be described with appropriate boundary conditions. According to this principle, the solution strategy is to consider two separated problems: the first problem corresponds to the description of the displacements on the plate due to dynamic loads applied on its upper surface, and the other corresponds to the description of the mechanical and electrical state of the piezoelectric patch under appropriate boundary conditions in Γ that model the influence of the reaction forces of the plate on the actuator or sensor. A graphical representation of this idea is given in Fig. 3.

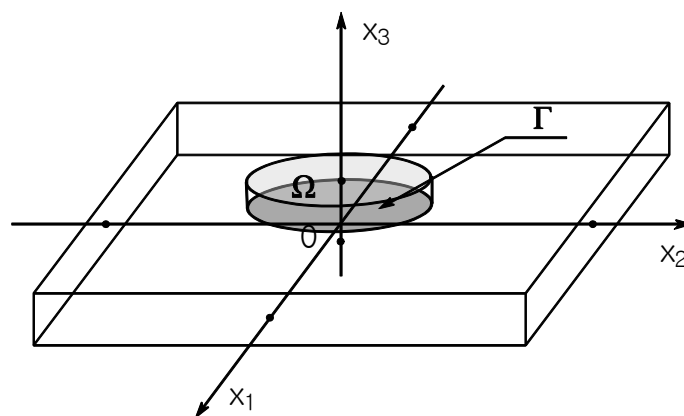


Fig. 2 Schematic representation and reference system of a piezoelectric patch bonded to a plate. The piezoelectric patch occupies a volume Ω and shares a common interface Γ with the plate

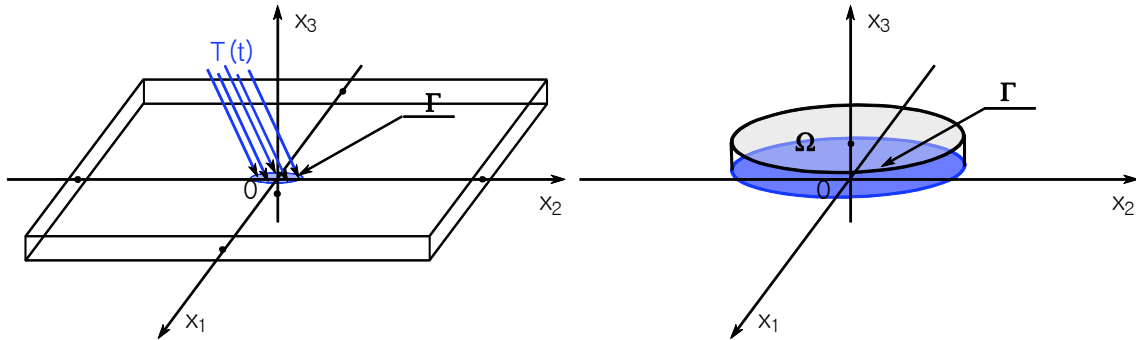


Fig. 3 The dynamic analysis of the plate and the piezoelectric patch is done separately. On the left side a plate is considered and the influence of the actuator or sensor is modeled as a dynamic load \mathbf{T} applied to the surface Γ . On the right side the piezoelectric transducer is considered and the reaction forces of the plate are modeled by specific boundary conditions on the surface Γ

It will be shown that the displacement field of the plate resulting from the applied loads can be accurately described with analytic expressions. To this end, we consider the governing equations and boundary conditions in the frequency domain. The novelty in the content of this work is the formulation of spectral methods in the frequency domain applied to bonded piezoelectric patches. In the following it is presented first how the conditions on the bonding surface Γ of the piezoelectric actuator and the plate are mathematically modeled. Then the respective discretization method using higher order finite element schemes is explained.

3. Wave propagation in isotropic plates

A homogeneous linear elastic isotropic plate of thickness d under a distribution of dynamic loads \mathbf{T} is considered, as shown in Fig. 3. The equation of motion corresponds to Navier's equation for a three dimensional isotropic body

$$(\lambda + \mu)\nabla\nabla \cdot \mathbf{u} + \mu\nabla^2\mathbf{u} = \rho\ddot{\mathbf{u}}. \quad (1)$$

The coefficients λ and μ are the elastic Lamé constants and ρ is the mass density. The unknown vector function $\mathbf{u} = \mathbf{u}(\mathbf{x}, t)$ corresponds to the vector of displacements depending on the position vector $\mathbf{x} = x_1\mathbf{e}_1 + x_2\mathbf{e}_2 + x_3\mathbf{e}_3$ and the temporal variable t . The unit vectors \mathbf{e}_1 , \mathbf{e}_2 and \mathbf{e}_3 are mutually perpendicular and have the direction of the three Cartesian coordinate axis. The symbols ∇ and ∇^2 denote the gradient and the Laplace's operator with respect to the spatial variable vector \mathbf{x} , respectively. An upper point represents the derivative with respect to time. The plate extends infinitely in the $x_1 - x_2$ plane and it is bounded by the top and bottom surfaces $x_3 = \pm d/2$. The influence of the external dynamical loads \mathbf{T} applied to the upper surface are introduced in the model through boundary conditions

$$\begin{aligned} \left[\mu(\nabla u_3 + \mathbf{u}_{,3}) + \lambda \nabla \cdot \mathbf{u} \mathbf{e}_3 \right]_{x_3=+d/2} &= \mathbf{T}, \\ \left[\mu(\nabla u_3 + \mathbf{u}_{,3}) + \lambda \nabla \cdot \mathbf{u} \mathbf{e}_3 \right]_{x_3=-d/2} &= 0. \end{aligned} \tag{2}$$

Here the notation $(\bullet)_{,3}$ stands for partial derivative with respect to x_3 .

3.1 Analytical approach

We consider the statement of this problem in the frequency domain. To this end, the Fourier transforms of the vector of displacements \mathbf{u} and the vector of loads \mathbf{T} are taken into account

$$\begin{aligned} \mathbf{u}^*(\bar{\mathbf{x}}, x_3; \omega) &= \int_{-\infty}^{+\infty} \mathbf{u}(\bar{\mathbf{x}}, x_3, t) e^{i\omega t} dt, \\ \mathbf{T}^*(\bar{\mathbf{x}}; \omega) &= \int_{-\infty}^{+\infty} \mathbf{T}(\bar{\mathbf{x}}, t) e^{i\omega t} dt. \end{aligned} \tag{3}$$

The vector $\bar{\mathbf{x}} = x_1 \mathbf{e}_1 + x_2 \mathbf{e}_2$ is provided with an upper bar to denote that it represents only in the in-plane components of the position vector $\mathbf{x} = \bar{\mathbf{x}} + x_3 \mathbf{e}_3$. The parameter ω is the circular frequency and i is the imaginary unit $\sqrt{-1}$. With this transformation in mind, the equation of motion in Eq. (1) is transformed in the frequency domain is as follows

$$(\lambda + \mu) \nabla \nabla \cdot \mathbf{u}^* + \mu \nabla^2 \mathbf{u}^* + \omega^2 \rho \mathbf{u}^* = 0. \tag{4}$$

In the frequency domain the derivation with respect to the temporal variable t is replaced by a multiplication with $i\omega$ and we obtain an equation where the circular frequency ω is introduced as a variable parameter. The boundary conditions remain essentially unchanged

$$\begin{aligned} \left[\mu(\nabla u_3^* + \mathbf{u}_{,3}^*) + \lambda \nabla \cdot \mathbf{u}^* \mathbf{e}_3 \right]_{x_3=+d/2} &= \mathbf{T}^*, \\ \left[\mu(\nabla u_3^* + \mathbf{u}_{,3}^*) + \lambda \nabla \cdot \mathbf{u}^* \mathbf{e}_3 \right]_{x_3=-d/2} &= 0. \end{aligned} \tag{5}$$

Integral expressions for the vector function \mathbf{u}^* that satisfy Eq. (4) and the boundary conditions Eq. (5) can be found in terms of \mathbf{T}^* using the concept of the response tensor also known as Green's tensor

$$\mathbf{u}^*(\bar{\mathbf{x}}, x_3; \omega) = \int_{\mathbb{R}^2} \mathbf{E}^*(\bar{\mathbf{x}} - \bar{\mathbf{x}}', x_3; \omega) \cdot \mathbf{T}^*(\bar{\mathbf{x}}'; \omega) d\bar{\mathbf{x}}'. \tag{6}$$

A closed-form analytical expression can be given for the frequency dependent response tensor \mathbf{E}^* . The procedure to derive those expressions can be found in the work of Vivar-Perez (2012) and it has some similarities to the procedure detailed by Karmazin *et al.* (2010, 2011) and von Ende *et al.* (2007). In this article only the two dimensional problem is considered. The analytic expression for the tensor \mathbf{E}^* for general three dimensional problems will be presented in the second part of the paper at hand.

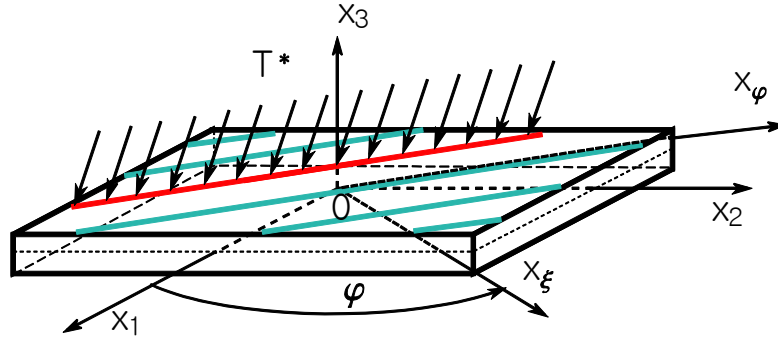


Fig. 4 Rotated reference system x_ξ, x_φ, x_3 and line distribution of loads applied on the surface of a plate, generating plane Lamb waves

3.2 Two-dimensional problem

It will be considered that the distribution of loads \mathbf{T} only depends on the spatial variable x_ξ , i.e., $\mathbf{T}^* = \mathbf{T}^*(x_\xi; \omega)$. The reference system given by the coordinates x_ξ, x_φ and x_3 is obtained from the Cartesian coordinate system determined by the coordinates x_1, x_2 and x_3 by a counterclockwise rotation about the x_3 axis by an angle φ , as shown in Fig. 4. In this case, the dependence on the variable x_φ is dropped from our model and the spatial dependence of \mathbf{u} on the position vector \mathbf{x} is reduced to the variables x_ξ and x_3 . An example of this configuration is given in Fig. 4.

Under these conditions Eq. (6) is transformed and results in

$$\mathbf{u}^*(\bar{\mathbf{x}}, x_3; \omega) = \int_{-\infty}^{+\infty} \mathbf{E}^*(x_\xi - x'_\xi, x_3; \omega) \cdot \mathbf{T}^*(x'_\xi; \omega) dx'_\xi, \quad (7)$$

where the matrix \mathbf{E}^* can be expressed as follows (Vivar-Perez, 2012)

$$\mathbf{E}^*(x_\xi, x_3; \omega) = \sum_{n=0}^{\infty} \left\{ \mathbf{E}^A(x_3; \xi_n^A, \omega) e^{i\xi_n^A x_\xi} + \mathbf{E}^S(x_3; \xi_n^S, \omega) e^{i\xi_n^S x_\xi} + \mathbf{E}^a(x_3; \xi_n^a, \omega) e^{i\xi_n^a x_\xi} + \mathbf{E}^s(x_3; \xi_n^s, \omega) e^{i\xi_n^s x_\xi} \right\}. \quad (8)$$

The matrix functions $\mathbf{E}^A, \mathbf{E}^S, \mathbf{E}^a$ and \mathbf{E}^s are the corresponding excitation matrices of the anti-symmetric Lamb modes, the symmetric Lamb modes, the anti-symmetric shear horizontal (SH) modes and the symmetric SH modes, respectively. In the two dimensional case the matrix functions can be given analytically as

$$\begin{aligned}
 \mathbf{E}^A(x_3; \xi, \omega) &= \frac{i}{2\mu \frac{\partial D_A}{\partial \xi}} \begin{pmatrix} N_{\xi\xi}^A & 0 & N_{\xi 3}^A \\ 0 & 0 & 0 \\ N_{3\xi}^A & 0 & N_{33}^A \end{pmatrix}, \quad \mathbf{E}^a(x_3; \xi, \omega) = \frac{i(-1)^n}{\mu\xi d} \sin \frac{(2n+1)\pi x_3}{d} \begin{pmatrix} 0 & 0 & 0 \\ 0 & 1 & 0 \\ 0 & 0 & 0 \end{pmatrix}, \\
 \mathbf{E}^S(x_3; \xi, \omega) &= \frac{i}{2\mu \frac{\partial D_S}{\partial \xi}} \begin{pmatrix} N_{\xi\xi}^S & 0 & N_{\xi 3}^S \\ 0 & 0 & 0 \\ N_{3\xi}^S & 0 & N_{33}^S \end{pmatrix}, \quad \mathbf{E}^s(x_3; \xi, \omega) = \frac{i(-1)^n}{\kappa_n \mu \xi d} \cos \frac{2n\pi x_3}{d} \begin{pmatrix} 0 & 0 & 0 \\ 0 & 1 & 0 \\ 0 & 0 & 0 \end{pmatrix}.
 \end{aligned} \tag{9}$$

In (9) we apply the convention $\kappa_0 = 2$ and $\kappa_n = 1$ for $n > 0$. The functions N in the entries of matrices \mathbf{E}^A and \mathbf{E}^S are as follows

$$\begin{aligned}
 N_{\xi\xi}^A(x_3; \xi, \omega) &= q \left[2\xi^2 \sin \frac{qd}{2} \sin px_3 - (\xi^2 - q^2) \sin \frac{pd}{2} \sin qx_3 \right], \\
 N_{\xi\xi}^S(x_3; \xi, \omega) &= q \left[-2\xi^2 \cos \frac{qd}{2} \cos px_3 + (\xi^2 - q^2) \cos \frac{pd}{2} \cos qx_3 \right], \\
 N_{3\xi}^A(x_3; \xi, \omega) &= -i\xi \left[2pq \sin \frac{qd}{2} \cos px_3 + (\xi^2 - q^2) \sin \frac{pd}{2} \cos qx_3 \right], \\
 N_{3\xi}^S(x_3; \xi, \omega) &= -i\xi \left[2\xi^2 \cos \frac{qd}{2} \sin px_3 + (\xi^2 - q^2) \cos \frac{pd}{2} \sin qx_3 \right], \\
 N_{\xi 3}^A(x_3; \xi, \omega) &= i\xi \left[(\xi^2 - q^2) \cos \frac{qd}{2} \sin px_3 + 2pq \cos \frac{pd}{2} \sin qx_3 \right], \\
 N_{\xi 3}^S(x_3; \xi, \omega) &= i\xi \left[(\xi^2 - q^2) \sin \frac{qd}{2} \cos px_3 + 2pq \sin \frac{pd}{2} \cos qx_3 \right], \\
 N_{33}^A(x_3; \xi, \omega) &= p \left[(\xi^2 - q^2) \cos \frac{qd}{2} \cos px_3 - 2\xi^2 \cos \frac{pd}{2} \cos qx_3 \right], \\
 N_{33}^S(x_3; \xi, \omega) &= p \left[-(\xi^2 - q^2) \sin \frac{qd}{2} \sin px_3 + 2\xi^2 \sin \frac{pd}{2} \sin qx_3 \right].
 \end{aligned} \tag{10}$$

and the functions D are given by the following expressions

$$\begin{aligned}
 D_A &= 4\xi^2 pq \cos \frac{pd}{2} \sin \frac{qd}{2} + (\xi^2 - q^2)^2 \sin \frac{pd}{2} \cos \frac{qd}{2} \\
 D_S &= 4\xi^2 pq \sin \frac{pd}{2} \cos \frac{qd}{2} + (\xi^2 - q^2)^2 \cos \frac{pd}{2} \sin \frac{qd}{2}
 \end{aligned} \tag{11}$$

with

$$p^2 = \frac{\omega^2}{c_1^2} - \xi^2, \quad q^2 = \frac{\omega^2}{c_2^2} - \xi^2, \quad c_1^2 = \frac{\lambda + \mu}{\rho}, \quad c_2^2 = \frac{\mu}{\rho}. \quad (12)$$

Thus, each mode has its corresponding excitation matrix. This formulation is convenient for applications, where only the contribution of one single mode is needed (Wilcox 2004). These matrices depend on the material, the geometry and the frequency and can be calculated beforehand, as well as the frequency-dependent wavenumbers $\xi_n^A, \xi_n^S, \xi_n^a$ and ξ_n^s . The wavenumbers ξ_n^A and ξ_n^S are the solutions of the Rayleigh-Lamb dispersion equations for anti-symmetric and symmetric Lamb modes, respectively, as

$$\begin{aligned} 4\xi^2 pq \cos \frac{pd}{2} \sin \frac{qd}{2} + (\xi^2 - q^2)^2 \sin \frac{pd}{2} \cos \frac{qd}{2} &= 0, \\ 4\xi^2 pq \sin \frac{pd}{2} \cos \frac{qd}{2} + (\xi^2 - q^2)^2 \cos \frac{pd}{2} \sin \frac{qd}{2} &= 0. \end{aligned} \quad (13)$$

The wavenumbers ξ_n^a and ξ_n^s corresponding to anti-symmetric and symmetric SH modes can be given explicitly as

$$\begin{aligned} \xi_n^a &= \sqrt{\frac{\omega^2}{c_2^2} - \frac{(2n+1)^2 \pi^2}{d^2}}, \\ \xi_n^s &= \sqrt{\frac{\omega^2}{c_2^2} - \frac{4n^2 \pi^2}{d^2}}. \end{aligned} \quad (14)$$

The dispersion relations in Eq. (13) constitute an implicit relation between the wavenumber ξ and the circular frequency ω , or the linear frequency $f = \omega/2\pi$. To find explicitly the values of ξ as a function of ω , or equivalently as a function of f , a numerical algorithm is applied. The algorithm used consists in tracking the curve branch corresponding to each mode in the $fd - \xi d$ plane, and it is based on a combination of Muller's method (Muller 1959) used to find complex roots of Eq. (13) and a procedure to trace implicit planar curves given by Yu *et al.* (2006).

Table 1 Material data for aluminum

Elastic Young's modulus	70GPa
Poisson's ratio	0.33
Mass density ρ	2700kg/m ³
Longitudinal velocity c_1	6197m/s
Transversal velocity c_2	3121m/s

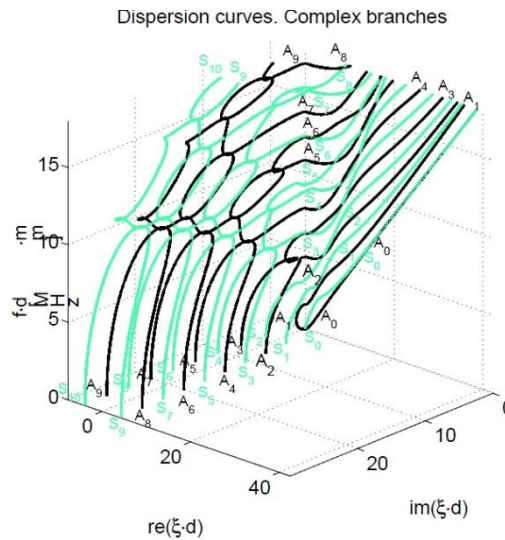


Fig. 5 Graphical representation of the wavenumber-frequency dependence corresponding to the first eleven symmetric and the first ten anti-symmetric Lamb modes of an aluminum plate. Curves corresponding to symmetric and anti-symmetric modes are represented in light and dark color, respectively

The value of the wavenumbers $\xi_n^A, \xi_n^S, \xi_n^a$ and ξ_n^s for each frequency are either complex or real. Complex values for the wavenumber correspond to decaying evanescent modes and real numbers to the propagating modes. It can be shown that for each frequency there is a finite number of propagating modes and the rest are evanescent. From Eq. (8) it follows that decaying evanescent modes have a small contribution to the value of the response matrix \mathbf{E}^* for values of x_ξ big enough. For this reason the sum in Eq. (8) is truncated for each x_ξ such that the absolute value of the contribution of the first neglected term is less than a prefixed tolerance.

Another point, worth mentioning, is that for the particular case of an isotropic plate, the values of these wavenumbers and the expressions for \mathbf{E}^* do not change with the direction of \mathbf{e}_ξ or the direction of propagation of the wave. Thus, in order to simplify notations we assume $\mathbf{e}_\xi = \mathbf{e}_1$ without losing generality. The same is not to be expected in anisotropic plates.

Fig. 5 illustrate the dependence between the wavenumbers and the frequency, the dispersion curves of the dependence of the wave numbers of the anti-symmetric and the symmetric Lamb modes, ξ_n^A and ξ_n^S and the linear frequency f is shown for an aluminum plate. The same can be seen in Fig. 6 for the wave numbers ξ_n^a and ξ_n^s of the anti-symmetric and the symmetric SH modes. The values of the material constants required for the calculation are given in Table 1.

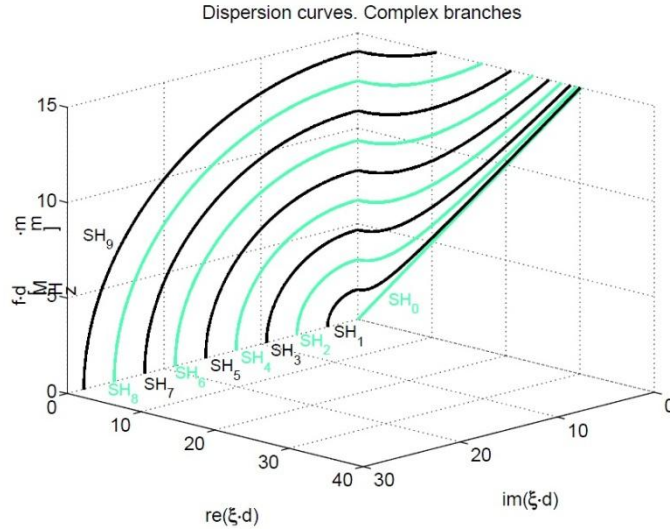


Fig. 6 Graphical representation of the wavenumber-frequency dependence corresponding to the first nine SH modes of an aluminum plate. Curves corresponding to symmetric and anti-symmetric modes are represented in light and dark color respectively

4. Modeling of bonded piezoelectric patches

After studying the displacement field of an infinite plate, a separate analysis is done with piezoelectric patches attached to it. The configuration and reference system corresponding to our model of a piezoelectric patch is shown in Fig. 1.

In piezoelectric materials the electrical and mechanical fields are coupled (Rose 2002, Royer and Dieulesaint 2000). The mechanical state is characterized by the vector of displacements \mathbf{u} , the strain tensor $\boldsymbol{\varepsilon}$ and the stress tensor $\boldsymbol{\sigma}$. The electrical state in a piezoelectric material is given by the electrical potential ϕ which is a scalar quantity, the electric field vector \mathbf{E} and the vector of electrical displacements \mathbf{D} .

4.1 Governing equations

The governing equations corresponding to the mechanical field are described by linearized relations between the vector of displacements \mathbf{u} and the second rank Cauchy strain tensor $\boldsymbol{\varepsilon}$

$$\boldsymbol{\varepsilon} = \frac{1}{2}(\nabla\mathbf{u} + \mathbf{u}\nabla) \tag{15}$$

and the balance equation in the elastic body in absence of body forces

$$\nabla \cdot \boldsymbol{\sigma} = \rho\ddot{\mathbf{u}}. \tag{16}$$

Consider that Γ_1 and Γ_2 are a disjoint partition of $\partial\Omega - \Gamma$, i.e., $\Gamma_1 \cap \Gamma_2 = \emptyset$ and

$\Gamma_1 \cup \Gamma_2 = \partial\Omega - \Gamma$, where $\partial\Omega - \Gamma$ is the set of points of the boundary of Ω excluding the points of Γ , cf. Fig. 7.

Assume that on Γ_1 the tractions \mathbf{T} are applied and on Γ_2 the displacements \mathbf{v} are prescribed. Then the boundary conditions corresponding to Γ_1 are defined as follows

$$\boldsymbol{\sigma} \cdot \mathbf{n}|_{\Gamma_1} = \mathbf{T}, \tag{17}$$

where \mathbf{n} is the outer normal vector to the surface Γ_1 . On Γ_2 the conditions are simply given by

$$\mathbf{u}|_{\Gamma_2} = \mathbf{v}. \tag{18}$$

Our initial conditions are the steady static state, i.e., the initial vector of displacements and velocities are equal to $\mathbf{0}$ when $t = 0$

$$\mathbf{u}(t=0) = \mathbf{0}, \quad \dot{\mathbf{u}}(t=0) = \mathbf{0} \tag{19}$$

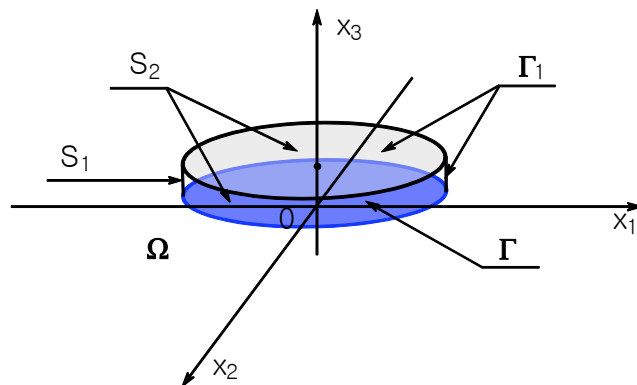


Fig. 7 Surfaces, Γ , Γ_1 , Γ_2 , S_1 and S_2 of $\partial\Omega$. The piezoelectric patch is electroded on the upper and lower surfaces S_2 and is not electroded on the lateral face S_1 . The lower surface Γ is shared by the plate and the piezoelectric transducer. The upper and lateral surfaces Γ_1 are traction free. In this case, there is no surface where the displacements are known or prescribed and the surface Γ_2 is an empty set ($\Gamma_2 = \emptyset$)

The influence of the electrical field is described by the equations of general electrostatics (Jackson 1998), consisting of the equations relating of the electrical potential and the electric field in the bounded domain Ω

$$\mathbf{E} = -\nabla\phi, \tag{20}$$

as well as the equation for the electrical displacement \mathbf{D} in absence of an internal distribution of

charges

$$\nabla \cdot \mathbf{D} = 0. \quad (21)$$

Conditions on the boundary $\partial\Omega$ are also taken into account. Let's take S_1 and S_2 such that $S_1 \cap S_2 = \emptyset$ and $S_1 \cup S_2 = \partial\Omega$ (see Fig. 7). The Neumann boundary conditions on S_1 , relating the normal flux of the electrical displacement vector to the charge density denoted by σ_e , are given as

$$\mathbf{D} \cdot \mathbf{n} = -\sigma_e. \quad (22)$$

The Dirichlet boundary conditions, prescribing a given electric potential γ on S_2 , are as follows

$$\phi|_{S_2} = \gamma. \quad (23)$$

For the electrical potential the following initial conditions are considered in the model

$$\phi(t=0) = 0, \quad \dot{\phi}(t=0) = 0. \quad (24)$$

We assume that our applications are within the limits of linear theory of piezoelectricity. Therefore the constitutive relations have the following form

$$\begin{aligned} \boldsymbol{\sigma} &= \mathbf{c} \cdot \boldsymbol{\varepsilon} - \mathbf{e} \cdot \mathbf{E}, \\ \boldsymbol{\sigma} &= \mathbf{e} \cdot \boldsymbol{\varepsilon} - \boldsymbol{\zeta} \cdot \mathbf{E}, \end{aligned} \quad (25)$$

where the fourth rank elasticity tensor \mathbf{c} , the third rank piezoelectric tensor \mathbf{e} and second rank dielectric tensor $\boldsymbol{\zeta}$ complete the set of coefficients of the linear constitutive law.

We make use of a Cartesian coordinate system to write the final governing equations of the linear piezoelectricity in terms of the electrical potential and the components of the vector of displacements. We substitute the equations of the electrical field Eq. (20), the linearized relations between the mechanical displacements and the mechanical strains Eq. (15) and the constitutive laws Eq. (25) in the balance equation Eq. (16) and the equation for the electrical displacement in Eq. (21) and obtain finally

$$\begin{aligned} c_{ijkl} u_{k,jl} + e_{lij} \phi_{,lj} &= \rho \ddot{u}_i, \\ e_{jkl} u_{k,jl} - \zeta_{lj} \phi_{,lj} &= 0. \end{aligned} \quad (26)$$

Einstein's summation convention regarding the sum over repeated indexes k , l and j is considered and an index j after a comma denotes a partial derivative with respect to the variable x_j . The equations Eq. (17), Eq. (18), Eq. (22) and Eq. (23) are rearranged and therefore, the boundary conditions can be stated in the following form

$$\begin{aligned}
 (c_{ijkl}u_{k,l} + e_{lij}\phi_{,l})n_j \Big|_{\Gamma_1} &= T_i, \\
 (e_{jkl}u_{k,l} - \zeta_{lj}\phi_{,l})n_j \Big|_{S_1} &= -\sigma_e, \\
 u_i \Big|_{\Gamma_2} &= v_i, \\
 \phi \Big|_{S_2} &= \gamma.
 \end{aligned}
 \tag{27}$$

4.2 Bonded piezoelectric patches

In order to introduce the boundary conditions corresponding to the bounding interface Γ the problem is transformed to the frequency domain. If we denote the Fourier transform of a function with a star as superscript and apply the direct Fourier transform in Eq. (3) to the governing equations of piezoelectricity in Eq. (26), we obtain the formulation of the problem in the frequency domain as

$$\begin{aligned}
 c_{ijkl}u_{k,lj}^* + e_{lij}\phi_{,lj}^* &= -\omega^2 \rho u_i^*, \\
 e_{jkl}u_{k,lj}^* - \zeta_{lj}\phi_{,lj}^* &= 0.
 \end{aligned}
 \tag{28}$$

In the bounding surface Γ not all the boundary conditions given in Eq. (27) apply. Therefore, this surface is separately considered. The application of the Fourier transform to the boundary conditions Eq. (27) results in

$$\begin{aligned}
 (c_{ijkl}u_{k,l}^* + e_{lij}\phi_{,l}^*)n_j \Big|_{\Gamma_1} &= T_i^*, \\
 (e_{jkl}u_{k,l}^* - \zeta_{lj}u_{k,l}^*)n_j \Big|_{S_1} &= -\sigma_e^*, \\
 u_i^* \Big|_{\Gamma_2} &= v_i^*, \\
 \phi^* \Big|_{S_2} &= \gamma.
 \end{aligned}
 \tag{29}$$

In the surface Γ the interaction between the piezoelectric patch and the plate has to be considered. An ideal bonding implies the continuity of the field of displacements and the distribution of tractions. If we denote by \mathbf{Q} the vector of reaction forces of the piezoelectric patch to the bonding surface Γ , we get

$$(c_{ijkl}u_{k,l}^* + e_{lij}\phi_{,l}^*)n_j \Big|_{\Gamma_1} + Q_i^* = 0.
 \tag{30}$$

On the interface Γ the displacements of the plate and the piezoelectric patch are the same. Thus, according to Eq. (6) we can make use of the relation between the Fourier transform of the displacements on the surface Γ of the plate and the Fourier transform of the applied loads \mathbf{Q} to finally obtain

$$\mathbf{u}^*(\bar{\mathbf{x}}, d/2; \omega) = \int_{\Gamma} \mathbf{E}^*(\bar{\mathbf{x}} - \bar{\mathbf{x}}', d/2; \omega) \mathbf{Q}^*(\bar{\mathbf{x}}'; \omega) d\bar{\mathbf{x}}' \quad \bar{\mathbf{x}} \in \Gamma.
 \tag{31}$$

Conditions given in Eqs. (30) and (31) constitute constraints that model the reaction of the plate to the movement or vibration of the bonded piezoelectric actuator on the surface Γ . Observe that the boundary condition in Eq. (31) includes the effect of the geometry of Γ through the region of integration, and the material properties as well as the thickness of the plate are taken into account by the factor \mathbf{E}^* in the integrand. Once the system of governing equations restricted to these boundary conditions is solved, we obtain a solution for the behavior of an isolated piezoelectric patch when it is perfectly bonded to the plate without the need to consider or analyze the behavior of any other point in the plate except for those contained in Γ . Nevertheless, after determining the traction distribution \mathbf{Q} defined on Γ , the displacements of any point in the plate due to the excitation of the piezoelectric patch or the reflection of the incident field due to piezoelectric or elastic obstacles can be determined through Eq. (6).

The Fourier transform of the distribution of the loads \mathbf{Q} in Γ , say \mathbf{Q}^* , can be determined once the system of partial differential equations in Eq. (28), constrained by the boundary conditions given by Eqs. (29)-(31) is solved. With that, the mechanical displacements of any point in the plate and in the bonded piezoelectric patch can be calculated in the frequency domain. To obtain the desired results in the time domain, the inverse Fourier transform must be applied to the results.

5. Chebyshev spectral analysis of bonded piezoelectric patches

In the following, the system of partial differential equations given by Eq. (28) together with the boundary conditions in Eqs. (29)-(31) is solved using spectral analysis.

5.1 The two-dimensional problem

The considered model describes a two-dimensional problem corresponding to a piezoelectric transducer bonded to an elastic plate as shown in Fig. 8. For the sake of simplicity, the equations resulting from the discretization of model are only presented for the reference domain $\Omega = [-1, 1]^2$. The same procedure can be analogously applied for a general quadrilateral shape if a coordinate transformation is considered.

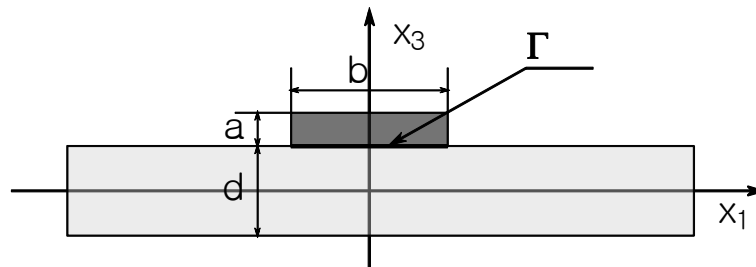


Fig. 8 Geometrical representation of a two-dimensional model corresponding to a piezoelectric patch bonded to a plate. The common interface between both bodies is Γ

Our choice for interpolation nodes within the interval $[-1,1]$ is the Chebyshev-Lobatto grid determined by the points

$$\xi_j = \cos \frac{j\pi}{N}, \quad j = 0, 1, \dots, N. \tag{32}$$

The Lagrange interpolation polynomials (also referred to as shape functions or cardinal functions) are computed in terms of the position of the nodes ξ_j with the following general formula

$$l_j^N(x) = \prod_{i=0, i \neq j}^N \frac{x - \xi_i}{\xi_j - \xi_i}. \tag{33}$$

The Chebyshev-Lobatto grid and its corresponding cardinal functions are illustrated in Fig. 9 for the case $N = 7$.

In the two-dimensional case, the nodes used for the interpolation procedure constitute a tensor product of the Chebyshev grid shown in Fig. 9. The distribution of the grid nodes in two dimensions is shown in Fig. 10. The polynomial degrees of the interpolation polynomials in the directions of x_1 and x_3 in the general case are denoted as N_1 and N_3 , respectively.

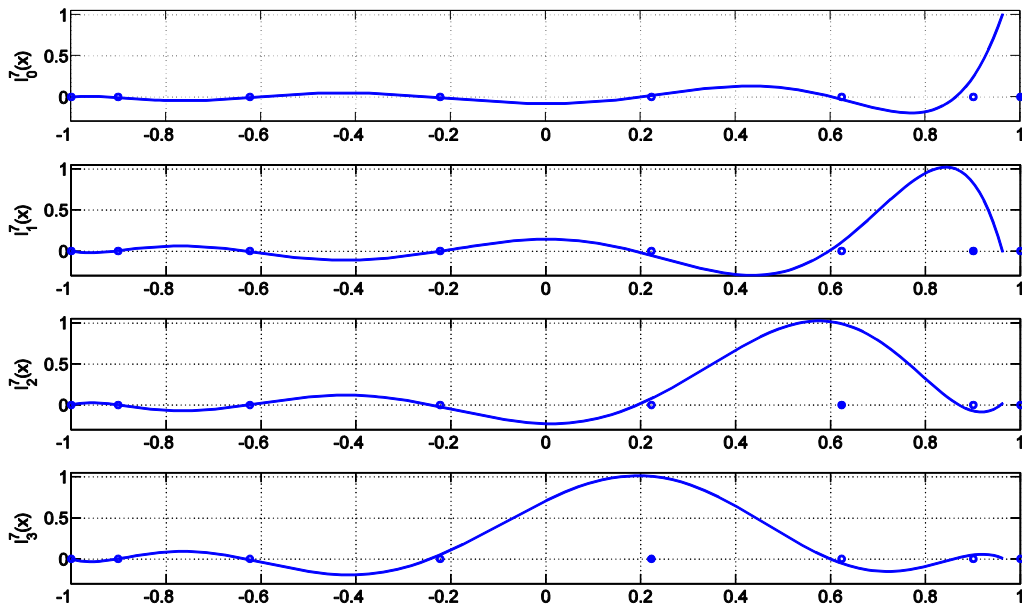


Fig. 9 Cardinal functions corresponding to a Chebyshev-Lobatto grid with $N = 7$. Only the functions $l_j^7(x)$ for $j = 0, 1, 2, 3$ are plotted from top to bottom. The other cardinal functions $l_j^7(x)$ for $j = 4, 5, 6, 7$ can be obtained by mirroring the given shape functions $l_j^7(x)$ for $j = 0, 1, 2, 3$ with respect to the axis $x = 0$

The approximation of each component of the unknown function of displacements u_k and the unknown electric potential ϕ is done according to,

$$\begin{aligned} u_k &\approx u_k^{N_1 N_3} = \sum_{n_1=0}^{N_1} \sum_{n_3=0}^{N_3} U_k^{n_1 n_3}(t) l_{n_1}^{N_1}(x_1) l_{n_3}^{N_3}(x_3), \\ \phi &\approx \phi^{N_1} = \sum_{n_1=0}^{N_1} \sum_{n_3=0}^{N_3} U_4^{n_1 n_3}(t) l_{n_1}^{N_1}(x_1) l_{n_3}^{N_3}(x_3). \end{aligned} \quad (34)$$

Consequently, the same approximation is used for the vector of reaction forces \mathbf{Q} on the interface Γ between the piezoelectric patch and the plate and is given by

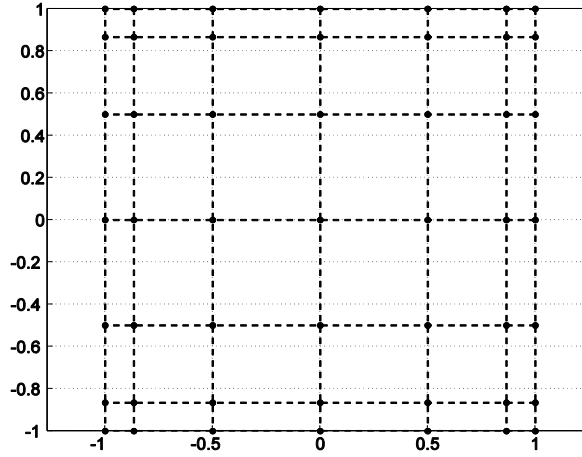


Fig. 10 Tensorial product of the Chebyshev-Lobatto grid in the two dimensional reference square $[-1, 1]^2$. The degree of polynomial interpolation is $N = 6$ in vertical and horizontal directions

$$Q_i \approx q_i^{N_1} = \sum_{n_1=0}^{N_1} Q_1^{n_1}(t) l_{n_1}^{N_1}(x_1), \quad (35)$$

Every triple (k, n_1, n_3) with $k = 1, 3, 4$; $n_1 = 0, 1, \dots, N_1$ and $n_3 = 0, 1, \dots, N_3$ is labeled with a different index n varying from 1 to $M = 3(N_1 + 1)(N_3 + 1)$. According to this all the values $U_k^{*n_1 n_3}$ can be arranged in the vector of degrees of freedom \mathbf{U}^* of size $M \times 1$. Consider first the case when the piezoelectric patch is not bonded to the plate, i.e., $\mathbf{Q}^* = 0$ in Eq. (30). Under this assumption, the result of substituting Eq. (34) in Eqs. (28)-(30) is a linear system of equations in \mathbf{U}^* for each frequency

$$\mathbf{K}^* \mathbf{U}^* = \mathbf{F}^*. \quad (36)$$

The column vector \mathbf{F}^* of size $M \times 1$ is the vector of loads and the square matrix \mathbf{K}^* of size M is the dynamic stiffness matrix

$$\mathbf{K}^* = \mathbf{K} + \omega^2 \mathbf{M}, \tag{37}$$

where \mathbf{K} and \mathbf{M} are respectively the mass and stiffness matrices of the original model.

When the piezoelectric patch is bonded to the plate we must consider the unknown reaction forces \mathbf{Q}^* and their relation with the displacements \mathbf{u}^* in the interface Γ given by Eq. (31). This is introduced in the discrete model in Eq. (36) by substituting Eq. (35) in Eq. (31). The integral resulting from the substitution is calculated using Clenshaw-Curtis quadrature formulas. For this choice of quadrature formula the quadrature nodes coincide with the nodes that are used for the discretization grid. If we denote by w_{n_1} , $n_1 = 0, \dots, N_1$ the weights of the quadrature formula, the equation resulting from the discretization of Eq. (31) is as follows

$$U_j^{*n_1 N_3} = \sum_{n \in I} w_{n_1} E_{ji}^* (x_1^{n_1} - x_1^{m_1}, d/2) Q_i^{*n_1}. \tag{38}$$

Denote by \mathbf{U}_I^* the column vector of the entries of \mathbf{U}^* that correspond to the displacements of nodes belonging to the interface Γ . Let us correspondingly arrange the values of $Q_i^{*n_1}$ in a column vector \mathbf{Q}^* . With this convection in mind Eq. (38) can be written in matrix form as follows

$$\mathbf{U}_I^* = \mathbf{E}^* \mathbf{Q}^*. \tag{39}$$

The entries of the matrix \mathbf{E}^* give a measure of the plate receptance to the loads \mathbf{Q}^* in Γ induced by the piezoelectric patch. The entry in the m -th row and the n -th column can be interpreted as the response in the degree of freedom m due to a unit force considered in the n -th entry of the vector \mathbf{Q}^* .

According to Eqs. (30) and (39), the final system of linear equations for each frequency ω can be written in terms of the dynamic stiffness matrix \mathbf{K}^* and the reaction matrix \mathbf{E}^* as follows

$$\begin{pmatrix} \mathbf{K}_{BB}^* & \mathbf{K}_{BI}^* \\ \mathbf{K}_{IB}^* & \mathbf{K}_{II}^* + (\mathbf{E}^*)^{-1} \end{pmatrix} \begin{pmatrix} \mathbf{U}_B^* \\ \mathbf{U}_I^* \end{pmatrix} = \begin{pmatrix} \mathbf{F}_B^* \\ \mathbf{F}_I^* \end{pmatrix}. \tag{40}$$

Solving this linear system of equations, the vector \mathbf{U}^* can be found and, with that, the mechanical and electrical state of the piezoelectric patch bonded to the structure is determined. The displacements at any point of the plate can be found once the vector \mathbf{Q}^* is determined through the following formula

$$\mathbf{Q}^* = \left\{ \left[\mathbf{K}_{II}^* - \mathbf{K}_{IB}^* (\mathbf{K}_{BB}^*)^{-1} \mathbf{K}_{BI}^* \right] \mathbf{E}^* + \mathbf{I} \right\}^{-1} \left\{ \mathbf{F}_I^* - \mathbf{K}_{IB}^* (\mathbf{K}_{BB}^*)^{-1} \mathbf{F}_B^* \right\}, \tag{41}$$

where \mathbf{I} is the identity matrix of the same size as \mathbf{E}^* . This expression is obtained if Eq. (39) is substituted in (40) and the resulting system of equations is solved for \mathbf{Q}^* .

6. Numerical results

In order to evaluate the reliability of the proposed methods, we consider a numerical experiment. The materials for the piezoelectric actuator and the plate are PIC-181 and aluminum, respectively. The material constants for both materials are listed in Tables 1 and 2.

The values of the geometrical parameter are $d = 2$ mm for the thickness of the plate and $a = 1$ mm denoting the thickness of the transducer and $b = 10$ mm representing the length of the piezoelectric patch, respectively (see Fig. 8). The surfaces of the plate are traction free, and the upper and the lower faces of the piezoelectric actuator are electroded. On the lower face of the actuator, it is considered that the potential ϕ vanishes and in the upper face it changes only with the temporal variable t according to a 3-cycle (n_0) sinus burst with a central frequency of $f_0 = 200$ KHz and with an amplitude of 50 V. Every point on the upper face has $\phi(t) = 50 \text{ V} \cdot p(t)$, where the time amplitude modulating function $p(t)$ is given by

$$p(t) = \frac{1}{2} [H(t) + H(n_0 / f_0 - t)] \sin^2 \frac{\pi f_0 t}{n_0} \sin 2\pi f_0 t, \quad (42)$$

and $H(t)$ is the Heaviside step function, i.e., $H(t) = 1$ if $t \geq 0$ and vanish otherwise.

A graph of $p(t)$ and the frequency content of its Fourier transform is depicted in Fig. 11.

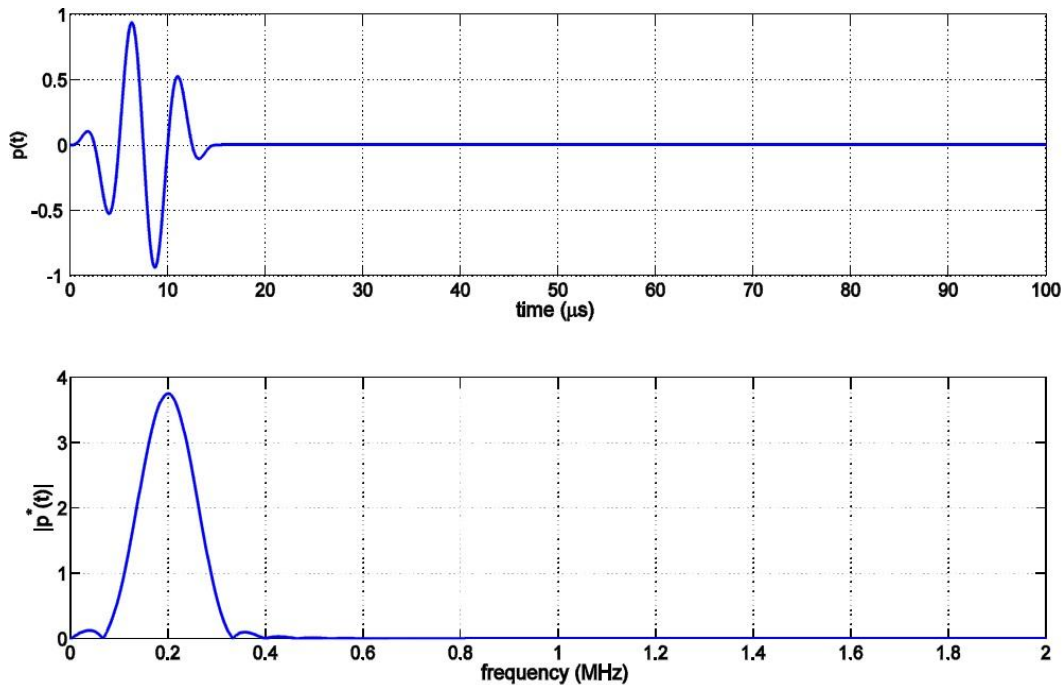


Fig. 11 The function $p(t)$, which corresponds to a three cycle sinus burst modulated by a Hann-window (above) and the absolute value of its Fourier transform $|p^*(t)|$ (below)

After determining the parameters that define the geometry of the problem and the boundary conditions, a discretization of the domain occupied by the piezoelectric material is introduced. For the benchmark example $N_1 = 20$ and $N_3 = 8$ were chosen as polynomial degrees in the direction of x_1 and x_3 , respectively. This amounts to a formulation with 567 degrees of freedom. Additionally, only the first 16 terms are considered in the infinite sum in Eq. (8) to build the dynamic reaction matrix \mathbf{E}^* according to Eqs. (38) and (39).

In Fig. 12, the simulation results of the motion of the piezoelectric transducer due to an applied electric potential difference are shown. With this method, the behavior of the bonded piezoelectric actuator can be analyzed by only considering the points contained on its domain. Nevertheless the effects of the reaction forces, caused by the elastic plate, on the behavior of the piezoelectric patch are observed. The effects of the reaction of the plate in the simplified model of the bonded patch are introduced by Eq. (31) or its discrete version given by Eq. (39). Observe that Eq. (39) can only be considered if the Green's response tensor of the plate has been previously determined, which constrains the application of the method only to those models where the response tensor is available.

Table 2 Values of the non-zero coefficients of the elasticity tensor \mathbf{c} , the piezoelectric tensor \mathbf{e} , the dielectric tensor ζ and the mass density ρ of PIC-181. The constant $\zeta_0 = 8.854187817620 \times 10^{-12}$ F/m is the vacuum permittivity

Elastic coefficients	(GPa)
$c_{1111} = c_{2222}$	152.30
c_{3333}	134.10
c_{1122}	89.09
$c_{1133} = c_{2233}$	85.42
c_{1212}	31.61
$c_{1313} = c_{2323}$	28.30
Piezoelectric coefficients	(N/Vm)
$e_{113} = e_{223}$	11.00
$e_{311} = e_{322}$	-4.50
e_{333}	14.70
Relative permittivity	
$\zeta_{11} / \zeta_0 = \zeta_{22} / \zeta_0$	1224
ζ_{33} / ζ_0	1135
Mass density	(kg/m ³)
ρ	7850

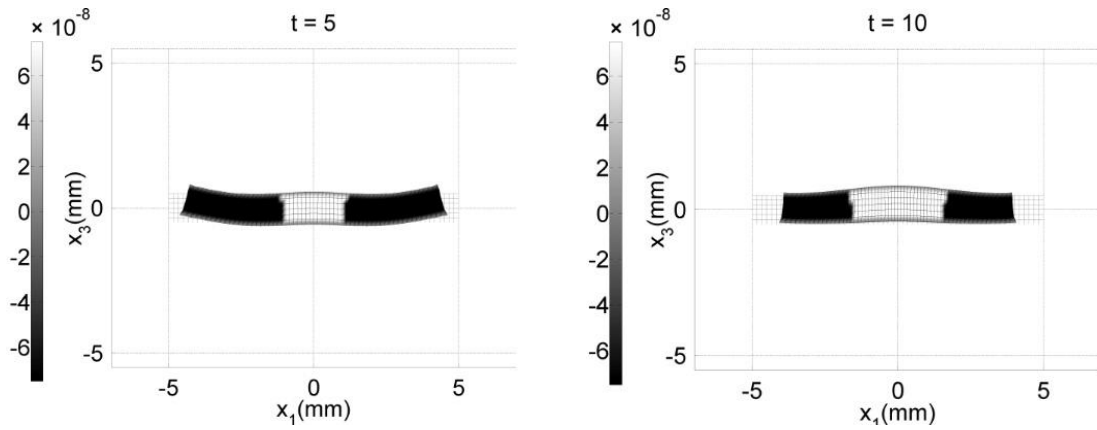


Fig. 12 Deformation of a piezoelectric actuator bonded to an elastic isotropic plate after $t = 5\mu s$ and $t = 10\mu s$. The contour plots represent the electrical potential in MV. The deformation scale factor is set to 2.0×10^4

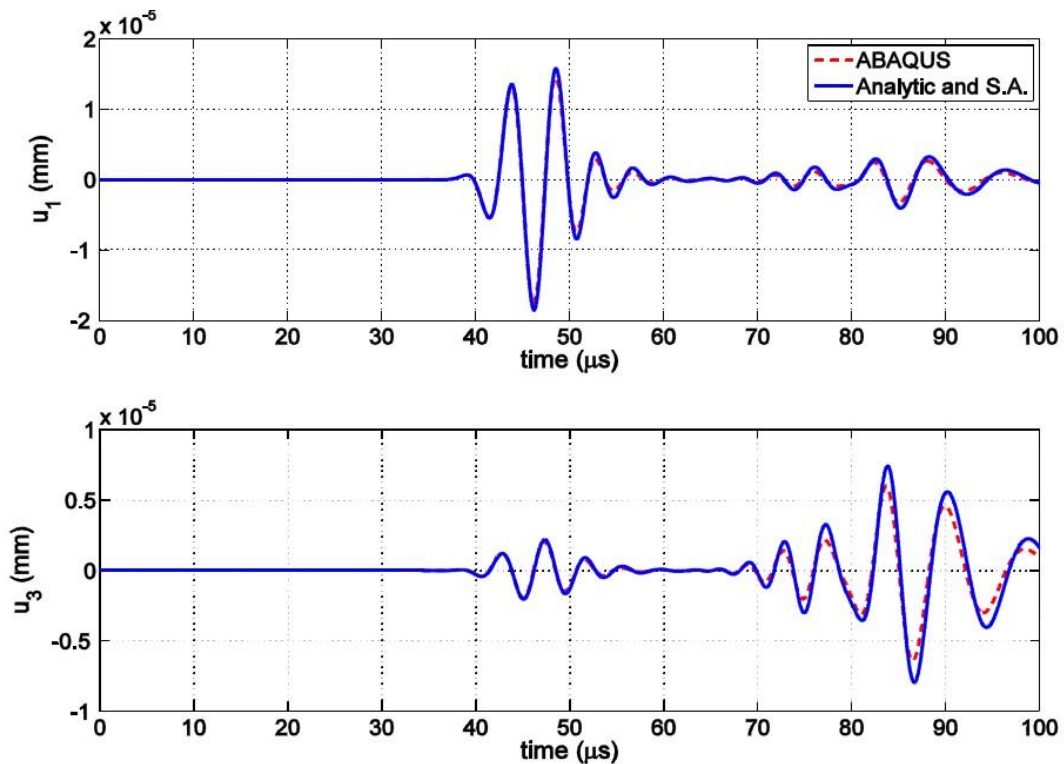


Fig. 13 Vertical and horizontal displacements at point $x_1 = 200$ mm on the surface of the plate excited by a piezoelectric actuator. The ABAQUS results are compared with the proposed method (combination of analytical and spectral methods)

As a way to verify the results, we calculated the displacements at some points in the plate that are not located at the bonding region of the piezoelectric actuator. We chose points located at $x_1 = 200$ mm and $x_1 = 245$ mm on the upper surface of the plate, i.e., $x_3 = 1$ mm. The results of the calculation were compared with finite element results calculated with ABAQUS. The FE-mesh is generated using rectangular quadratic elements with the element size of 0.25mm. Both results agree very well as can be seen in Figs. 13 and 14.

The same analysis is applied to study the behavior of piezoelectric sensors. We considered the case when a piezoelectric patch with the same dimensions as the actuator is attached to the surface of the plate in the region delimited by the points $x_1 = 195$ mm and $x_1 = 205$ mm. In Fig. 15 we plotted snapshots of the piezoelectric patch in at different times $t = 80\mu s$ and $t = 85\mu s$, where the piezoelectric sensor is under the influence of the traveling A_0 mode. The snapshots are shown in Fig. 15. Here it is clear to see that although the piezoelectric sensor is considered separately the effects of the traveling A_0 mode in terms of deformation and electric potential are to be seen.

This shows the capability of the method to describe the piezoelectric behavior of a piezoelectric sensor/actuator system bonded to a plate without considering any point within or the discretization of the plate, except for the points that belong to the bonding surfaces. This is very advantageous regarding the simulations of Lamb waves excited by piezoelectric transducers with applications to non-destructive testing. The number of degrees of freedom of the system and the calculation effort reduces significantly and it simplifies the analysis of the behavior of the sensor due to effect of the signals emitted by the actuators.

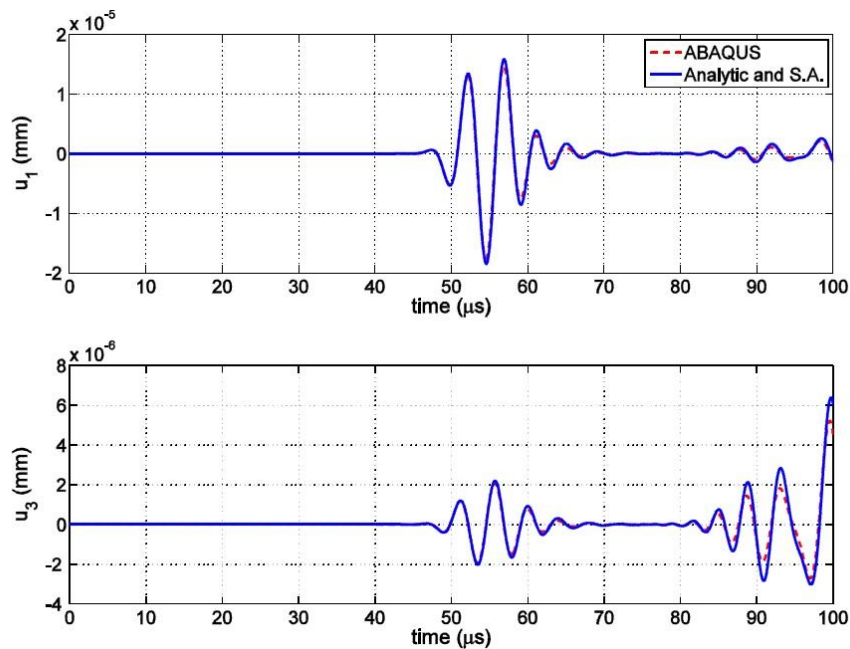


Fig. 14 Vertical and horizontal displacements at point $x_1 = 245$ mm on the surface of the plate excited by a piezoelectric actuator. The ABAQUS results are compared with the proposed method (combination of analytical and spectral methods)

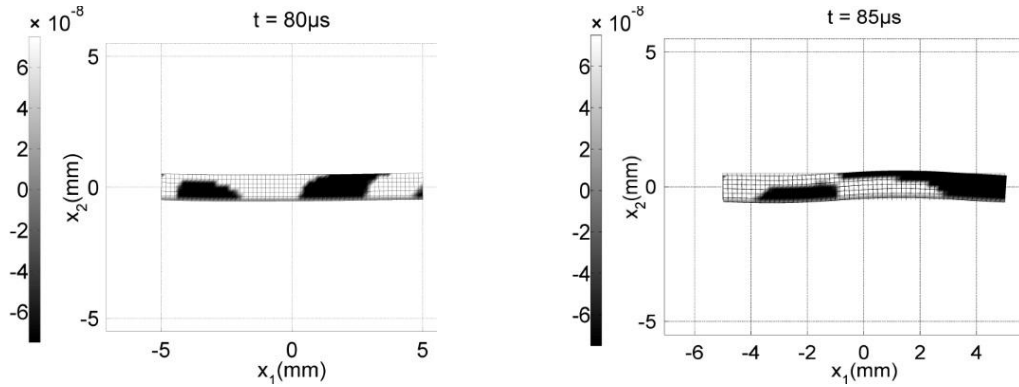


Fig. 15 The deformation of a piezoelectric sensor bonded to an elastic isotropic plate on the upper face $195\text{mm} \leq x_1 \leq 205\text{mm}$ mm after $t = 80\mu\text{s}$ and $t = 85\mu\text{s}$ s of the excitation signal. The contour plots represent the electrical potential in MV. The deformation scale factor is set to 2.0×10^4

7. Conclusions

In this work the use of analytical and spectral methods has been used to model Lamb waves in isotropic plates induced by piezoelectric transducers. The capability of the method to model the behavior of wave propagation in elastic plates as well as the effects of piezoelectric transducers attached to the structure is shown.

The spectral analysis was utilized to model piezoelectric transducers (actuators and sensors). A mathematical model to describe the mechanical and electrical fields of piezoelectric transducers bonded to an elastic isotropic plate is given and its accuracy is verified. With help of the spectral analysis combined with analytical methods, the reaction forces of the plate to a vibrating transducer are also taken into account. Thus, a method to study piezoelectric transducers bonded to a structure is provided without considering any other region of the plate other than the bonding surface. The time-dependent displacements at any point of the plate are calculated using this formulation.

The analytical methods applied here to model the propagation of elastic guided waves in plates have many advantages in comparison with other methods used for the same purposes. In regards to finite element or finite difference based methods, the analytical formulation presented here has the advantage that there is no need to discretize the complete domain of the plate to obtain the solution of displacements at any point of an infinite plate. As a matter of fact, the history of displacements at a certain point of the plate can be calculated without considering the displacement at neighboring points and no assumption about the number of elements/nodes per wave length has to be taken into account. This results in a huge improvement in terms of the calculation time and the memory storage requirements. The time history of displacements is calculated using the fast Fourier transform algorithm. Therefore no numerical dispersion is introduced as in cases where time domain simulations are made with an iterative time integration scheme like central differences or Runge-Kutta. An important advantage is that with analytical methods in the frequency domain the contribution of each mode to the displacement field can be separately analyzed and studied. This is very useful when only propagating modes are considered and all

evanescent modes are neglected, which is very convenient if the point considered to monitor the signal produced by the actuator is relatively far away from the source of excitation. This is a feature shared by analytical and semi-analytical approaches, but not by finite element and finite difference based approaches. With analytical approaches we are capable to model plates of infinite dimensions. Reflections from the boundaries of the plate are neglected in the current model. This is very useful when only the information of the reflections from damages are investigated or in the case that big plate structures are considered and the amplitudes of the sending waves are very small before the reflections. With classical methods used in time domain simulations, the dimensions of the model must be necessarily finite and they have to be coupled with another sort of discretization on the boundary such as boundary finite elements, infinite elements or artificial damping elements in order to eliminate the reflections at the boundary.

Anisotropy and stratified materials obtained by an arrangement of phases of different properties of orientation is something that is not considered in this work. Anisotropic and composite plates can also be modeled following a similar philosophy. Some work in this direction has already been done and some hybrid techniques have also been developed. In this case also the initial equations have to be changed in order to achieve this goal. This is work in progress and will be reported in forthcoming publications.

Acknowledgements

The authors would like to thank the German Research Foundation (DFG) and all project partners (PAK 357) for their support (GA 480/13-2). Additionally, the support received by the postgraduate program of the German Federal State of Saxony-Anhalt is also gratefully by the second author acknowledged.

References

- Achenbach, J.D. (1973), *Wave propagation in elastic solids*, (Eds. H.A. Lauwerier and W. T. Koiter), *North-Holland Series in Applied Mathematics and Mechanics*, volume 16, North Holland, Amsterdam, The Netherlands.
- Achenbach, J.D. (1998), "Lamb waves as thickness vibrations superimposed on a membrane carrier wave", *J. Acoust. Soc. Am.*, **103**(5), 2283-2286.
- Achenbach, J.D. (1999), "Wave motion in an isotropic elastic layer generated by a time-harmonic point load of arbitrary direction", *J. Acoust. Soc. Am.*, **106**(1), 83-90.
- Achenbach, J.D. and Xu, Y. (1999), "Use of elastodynamic reciprocity to analyze point-load generated axisymmetric waves in a plate", *Wave Motion*, **30**(1), 57-67.
- Achenbach, J.D. (2000), "Quantitative nondestructive evaluation", *Int. J. Solids Struct.*, **37**(1, 2), 13-27.
- Achenbach, J.D. (2003), *Reciprocity in elastodynamics*, Cambridge Monographs on Mechanics, Cambridge University Press, Cambridge, United Kingdom.
- Ahmad, Z.A.B. (2011), *Numerical simulations of waves in plates using a semi-analytical finite element method*, Technical report: *Fortschritt-Berichte VDI*, Number 437 in Reihe 20-Rechnerunterstützte Verfahren. VDI Verlag.
- Ahmad, Z.A.B., Vivar-Perez, J.M., Willberg, C. and Gabbert, U. (2009), "Lamb wave propagation using wave finite element method", *PAMM- Proc. Appl. Math. Mech.*, **9**, 509-510.
- Bartoli, I., Marzania, A., Lanza di Scalea, F. and Violab, E. (2006), "Modeling wave propagation in damped waveguides of arbitrary cross-section", *J. Sound Vib.*, **295**(3-5), 685-707.

- Bonnet, M. and Constantinescu, A. (2005), "Inverse problems in elasticity", *Inverse Probl.*, **21**(2), 1-50.
- Boyd, J.P. (2000), *Chebyshev and fourier spectral methods* (2nd Ed.), Dover, New York, USA.
- Chakraborty, A. and Gopalakrishnan, S. (2004), "Wave propagation in inhomogeneous layered media: solution of forward and inverse problems", *Acta Mech.*, **169**, 153-185.
- Chang, Z. and Mal, A. (1999), "Scattering of Lamb waves from a rivet hole with edge cracks", *Mech. Mater.*, **31**(3), 197-204.
- Delsanto, P.P., Whitcombe, T., Chaskelis, H.H. and Mignogna, R.B. (1992), "Connection machine simulation of ultrasonic wave propagation in materials. I: The one-dimensional case", *Wave Motion*, **16**(1), 65-80.
- Delsanto, P.P., Schechter, R.S., Chaskelis, H.H., Mignogna, R.B. and Kline, R. (1994), "Connection machine simulation of ultrasonic wave propagation in materials. II: The two-dimensional case", *Wave Motion*, **20**(4), 295-314.
- Delsanto, P.P., Schechter, R.S. and Mignogna, R.B. (1997), "Connection machine simulation of ultrasonic wave propagation in materials III: The three-dimensional case", *Wave Motion*, **26**(4), 329-339.
- Doyle, J.F. (1997), *Wave propagation in structures: spectral analysis using fast discrete Fourier transform. 2 edition*, Mechanical Engineering Series, Springer, New York, USA.
- Duczek, S., Willberg, C., Schmicker, D. and Gabbert, U. (2012), "Development, validation and comparison of higher order finite element approaches to compute the propagation of Lamb waves efficiently", *Key Eng. Mater.*, **518**, 95-105.
- Fornberg, B. (1998), *A practical guide to pseudospectral methods*, (Eds. P.G. Ciarlet, A. Iserles, R.V. Kohn, and M.H. Wright), Cambridge Monographs on Applied and Computational Mathematics, Cambridge University Press, United Kindom.
- Galàn, J.M. and Abascal, R. (2002), "Numerical simulation of Lamb wave scattering in semi-infinite plates", *Int. J. Numer. Meth. Eng.*, **53**(5), 1145-1173.
- Gazis, D.C. (1958), "Exact analysis of the plane-strain vibrations of thick-walled hollow cylinders", *J. Acoust. Soc. Am.*, **30**(8), 786-794.
- Giurgiutiu, V. (2005), "Tuned lamb wave excitation and detection with piezoelectric wafer active sensors for structural health monitoring", *J. Intel. Mat. Syst. Str.*, **16**, 291-305.
- Glushkov, E.V., Glushkova, N.V., Seemann, W. and Kvasha, O.V. (2006). "Elastic wave excitation in a layer by piezoceramic patch actuators", *Acoust. Phys.*, **52**(4), 398-407.
- Glushkov, Y.V., Glushkova, N.V. and Krivonos, A.S. (2010), "The excitation and propagation of elastic waves in multilayered anisotropic composites", *J. Appl. Math. Mech.*, **74**(3), 297-305.
- Gomilko, A.M., Gorodetskaya, N.S. and Meleshko, V.V. (1991), "Longitudinal Lamb waves in a semi-infinite elastic layer", *Int. J. Appl. Mech.*, **27**(6), 577-581.
- Gopalakrishnan, S. and Mitra, M. (2010), *Wavelet methods for dynamical problems: with application to metallic, composite, and nano-composite structures*, CRC Press Inc, Florida, USA.
- Gopalakrishnan, S., Chakraborty, A. and Mahapatra, D.R. (2008), *Spectral finite element method*, (Ed. K.J. Bathe), Computational Fluid and Solid Mechanics, volume XIV. Springer, New York, USA.
- Graff, K.F. (1975), *Wave motion in elastic solids*, Oxford University Press, London, United Kindom.
- Hayashi, T. and Kawashima, K. (2002), "Multiple reflections of Lamb waves at a delamination", *Ultrasonics*, **40**(1-8), 193-197.
- Holden, A. (1951), "Longitudinal modes of elastic waves in isotropic cylinders and slabs", *Bell Syst. Technical J.*, **30**(4), 956-969.
- Huang, H., Pamphile, T. and Derriso, M. (2008), "The effect of actuator bending on Lamb wave displacement fields generated by a piezoelectric patch", *Smart Mater. Struct.*, **17**(5), 1-13.
- Jackson, J.D. (1998), *Classical electrodynamics* (3rd Ed.), John Wiley & Sons, Inc. New York, USA.
- Jin, J., Quek, S.T. and Wang, Q. (2003), "Analytical solution of excitation of Lamb waves in plates by inter-digital transducers", *P. Roy. Soc. Lond. A*, **459**(2033), 1117-1134.
- Karmazin, A., Kirillova, E., Seemann, W. and Syromyatnikov, P. (2010), "Modelling of 3d steady-state oscillations of anisotropic multilayered structures applying the Green's functions", *Adv. Theor. Appl. Mech.*, **3**(9), 425-445.

- Karmazin, A., Kirillova, E., Seemann, W. and Syromyatnikov, P. (2011), "Investigation of Lamb elastic waves in anisotropic multilayered composites applying the Green's matrix", *Ultrasonics*, **51**(1), 17-28.
- Kudela, P. and Ostachowicz, W.M. (2008), "Wave propagation modelling in composite plates", *Appl. Mech. Mater.*, **9**, 89-104.
- Kudela, P. and Ostachowicz, W. M. (2009), "3D time-domain spectral elements for stress waves modelling", *J. Physics*, **181**(1), 1-8.
- Lamb, H. (1917), "On waves in an elastic plate", *P. Roy. Soc. A*, **93**, 114-128.
- Lee, B.C. and Staszewski, W.J. (2003a), "Modelling of Lamb waves for damage detection in metallic structures: Part I. Wave propagation", *Smart Mater. Struct.*, **12**(5), 804-814.
- Lee, B.C. and Staszewski, W.J. (2003b), "Modelling of Lamb waves for damage detection in metallic structures: Part II. Wave interactions with damage", *Smart Mater. Struct.*, **12**(5), 815-824.
- Leonard, K.R., Malyarenko, E.V. and Hinders, M. K. (2002), "Ultrasonic Lamb wave tomography", *Inverse Probl.*, **18**(6), 1795-1808.
- Liu, G.R. (2002), "A combined finite element/strip element method for analyzing elastic wave scattering by cracks and inclusions in laminates", *Comput. Mech.*, **28**(1), 76-81.
- Love, A.E. (1911), *Some problems of geodynamics*, Cambridge University Press, Cambridge, United Kindom.
- Loveday, P.W. (2007), "Analysis of piezoelectric ultrasonic transducers attached to waveguides using waveguide finite elements", *IEEE T. Ultrason. Ferr.*, **54**(10), 2045-2051.
- Lu, Y., Wang, X., Tang, J. and Ding, Y. (2008), "Damage detection using piezoelectric transducers and the Lamb wave approach: II. Robust and quantitative decision making", *Smart Mater. Struct.*, **17**(2), 025034, doi:10.1088/0964-1726/17/2/025034.
- Lyon, R.H. (1955), "Response of an elastic plate to localized driving forces", *J. Acoust. Soc. Am.*, **27**(2), 259-265.
- Mindlin, R.D. (1951), "Thickness-shear and flexural vibrations of crystal plates", *J. Appl. Phys.*, **22**(3), 316-323.
- Mindlin, R.D. and Medick, M.A. (1959), "Extensional vibrations of elastic plates", *J. Appl. Mech. - TASME*, **26**, 561-569.
- Mindlin, R.D. (1960), *Waves and vibrations in isotropic elastic plates*, (Eds. J.N. Goodier and N.J. Hoff) First Symposium on Naval Structural Mechanics, 1958. Pergamon, Oxford .
- Morvan, B., Wilkie-Chancellier, N., Duflo, H., Trinel, A. and Duclos, J. (2003), "Lamb wave reflection at the free edge of a plate", *J. Acoust. Soc. Am.*, **113**(3), 1417-1425.
- Muller, D.E. (1959), "A method for solving algebraic equations using an automatic computer", *Math. Comput.*, **10**(56), 208-215.
- Onoe, M.A. (1955), *A study of the branches of the velocity-dispersion equations of elastic plates and rods*, Technical report: Report Joint Committee on Ultrasonics of the Institute of Electrical Communication engineers and the Acoustical society of Japan.
- Osborne, M.F.M. and Hart, S.D. (1945), "Transmission, reflection, and guiding of an exponential pulse by a steel plate in water. I. theory", *J. Acoust. Soc. Am.*, **17**(1), 1-18.
- Ostachowicz, W.M., Kudela, P., Krawczuk, M. and Zak, A. (2012), *Guided waves in structures for SHM: the time-domain spectral element method*, John Wiley & Sons, Ltd, United Kindom.
- Peng, H., Meng, G. and Li, F. (2009), "Modeling of wave propagation in plate structures using three-dimensional spectral element method for damage detection", *J. Sound Vib.*, **320**, 942-954.
- Raghavan, A. and Cesnik, C.E.S. (2004), "Modeling of piezoelectric-based Lamb wave generation and sensing for structural health monitoring", *Proc. SPIE*, **5391**, 419-430.
- Raghavan, A. and Cesnik C.E.S. (2007), "Review of guided-wave structural health monitoring", *Shock Vib.*, **39**(2), 91-114.
- Rayleigh, L. (1885), "Waves propagated along the plane surface of an elastic solid", *Proc. London Math. Soc.*, **20**, 225-234.
- Rose, J.L. (2002), "A baseline and vision of ultrasonic guided wave inspection potential", *J. Press. Vessel T. - ASME*, **124**(3), 273-282.

- Royer, D. and Dieulesaint, E. (2000), *Elastic waves in solids I: free and guided propagation*, Springer, Berlin, Germany.
- Sirohi, J. and Chopra, I. (2000), "Fundamental understanding of piezoelectric strain sensors", *J. Intel. Mater. Syst. Str.*, **11**, 246-247.
- Su, Z. and Ye, L. (2009), *Identification of damage using Lamb waves. from fundamentals to applications*, (Eds. F. Pfeiffer and P. Wriggers), *Lecture Notes in Applied and Computational Mechanics*, volume 48, Springer, London, United Kingdom.
- Sun, J.H. and Wu, T.T. (2009), "A Lamb wave source based on the resonant cavity of phononic-crystal plates", *IEEE T. Ultrason. Ferr.*, **59**(1), 121-128.
- Tian, J., Gabbert, U., Berger, H., and Su, X. (2004), "Lamb wave interaction with delaminations in CFRP laminate", *Comput. Mater. Continua*, **1**(4), 327-336.
- Trefethen, L.M. (2000), *Spectral methods in MATLAB*. SIAM, USA.
- Velichko, A. and Wilcox, P.D. (2007), "Modeling the excitation of guided waves in generally anisotropic multilayered media", *J. Acoust. Soc. Am.*, **121**(1), 60-69.
- Viktorov, I.A. (1967), *Rayleigh and Lamb waves: physical theory and applications*, Plenum Press, New York, USA.
- Vivar-Perez, J.M. (2012), *Analytical and spectral methods for the simulation of elastic waves in thin plates*, Technical Report: Number 441 in Reihe 20, Fortschritt- Berichte VDI. VDI Verlag.
- Vivar-Perez, J. M., Willberg, C. and Gabbert, U. (2009a), "Simulation of piezoelectric induced Lamb waves in plates", *PAMM-Proc. Appl. Math. Mech.*, **9**, 503-504.
- Vivar-Perez, J.M., Willberg, C. and Gabbert, U. (2009b), "Simulation of piezoelectric Lamb waves in plate structures", *Proceedings of the International Conference on Structural Engineering Dynamics. ICEDyn Ericeira, Portugal. 22.-24. June*.
- von Ende, S., Schäfer, I. and Lammering, R. (2007), "Lamb wave excitation with piezoelectric wafers - an analytical approach", *Acta Mech.*, **193**(3-4), 141-150.
- Von Ende, S. and Lammering, R. (2007), "Investigation on piezoelectrically induced Lamb wave generation and propagation", *Smart Mater. Struct.*, **16**(5), 1802-1809.
- von Ende, S. and Lammering, R. (2009), "Modeling and simulation of Lamb wave generation with piezoelectric plates", *Mech. Adv. Mater. Struct.*, **16**(3), 188-197.
- Wang, X., Lu, Y. and Tang, J. (2008), "Damage detection using piezoelectric transducers and the Lamb wave approach: I. system analysis", *Smart Mater. Struct.*, **17**(2), 025033, doi:10.1088/0964-1726/17/2/025033.
- Wilcox, P. (2004), "Modeling the excitation of Lamb and SH waves by point and line sources", *AIP Conference Proc.*, **700**, 206-213.
- Willberg, C., Vivar-Perez, J.M. and Gabbert, U. (2009a), "Lamb wave interaction with defects in homogeneous plates", *Proceedings of the International Conference on Structural Engineering Dynamics (ICEDyn)*, Ericeira, Portugal. 22.-24. June.
- Willberg, C., Vivar-Perez, J.M., Ahmad, Z. and Gabbert, U. (2009b), "Simulation of piezoelectric induced Lamb wave motion in plates", *Proceedings of the 7th International Workshop on Structural Health Monitoring 2009: From System Integration to Autonomous Systems*.
- Willberg, C., Duczek, S., Vivar-Perez, J.M., Schmicker, D. and Gabbert, U. (2012), "Comparison of different higher order finite element schemes for the simulation of Lamb waves", *Comput. Meth. Appl. Mech. Eng.*, **241-244**, 246-261.
- Xu, B., Shen, Z., Ni, X. and Lu, J. (2004), "Numerical simulation of laser-generated ultrasound by the finite element method", *J. Appl. Phys.*, **95**(4), 2116- 2121.
- Yu, Z.S., Cai, Y.Z., Oh, M.J., Kim, T.W. and Peng, Q.S. (2006), "An efficient method for tracing planar implicit curves", *J. Zhejiang University Sci. A*, **7**(7), 1115-1123.